Materials Research Bulletin 48 (2013) 3149–3156

Contents lists available at SciVerse ScienceDirect

Materials Research Bulletin

journal homepage: www.elsevier.com/locate/matresbu

High stable suspension of magnetite nanoparticles in ethanol by using sono-synthesized nanomagnetite in polyol medium

Tahereh Rohani Bastami, Mohammad H. Entezari *

Department of Chemistry, Ferdowsi University of Mashhad, 91775 Mashhad, Iran

ARTICLE INFO

Article history:
Received 4 March 2012
Received in revised form 23 December 2012
Accepted 26 April 2013
Available online 10 May 2013

Keywords:
A. Magnetic materials
B. Chemical synthesis
C. Infrared spectroscopy
D. Surface properties

ABSTRACT

The sonochemical synthesis of magnetite nanoparticles was carried out at relatively low temperature (80 °C) in ethylene glycol (EG) as a polyol solvent. The particle size was determined by transmission electron microscopy (TEM). The magnetite nanoparticles with an average size of 24 nm were composed of small building blocks with an average size of 2–3 nm and the particles exhibited nearly spherical shape. The surface characterization was investigated by using Fourier transform infrared (FTIR) spectroscopy, X-ray photoelectron spectroscopy (XPS), and thermogravimetric analysis (TGA). The stability of magnetite nanoparticles was studied in ethanol as a polar solvent. The nanoparticles showed an enhanced stability in ethanol which is due to the hydrophilic surface of the particles. The colloidal stability of magnetite nanoparticles in ethanol was monitored by UV–visible spectrophotometer. According to the results, the nanoparticles synthesized in 30 min of sonication with intensity of 35 W/cm^2 (50%) led to a maximum stability in ethanol as a polar solvent with respect to the other applied intensities. The obtained magnetite nanoparticles were stable for more than12 months.

1. Introduction

Stable suspension of magnetic nanoparticles in different polar solvents has a great attention due to the broad application from medical [1,2] such as magnetic drug targeting [3] and magnetic resonance imaging contrast agent [4] to industrial application like pressure seals and rotary shaft seals [5]. The preparation of a stable and monodisperse dispersion is a crucial parameter in improving the quality of a suspension. In order to develop the suspension stability of nanoparticles, it is required to add some functional groups on the dispersing nanoparticles. Two approaches were found to obtain colloidally stable suspensions of the magnetic nanoparticles: (1) electrostatic interaction between nanoparticles, and (2) steric stabilization effects introduced by proper surface ligands. To date several synthesis routs were carried out for the synthesis of magnetic nanoparticles with different structures and composites such as co-precipitation [6], microemulsion [7], and solvothermal [8]. Several approaches have also been introduced for the suspension stability of magnetic nanoparticles in nonpolar solvents [8–10].

To make magnetic nanoparticles suitable for biological applications, the hydrophobic surface needs to be replaced by a hydrophilic and biocompatible functional coating. There are different methods for obtaining stable suspension of hydrophilic magnetic nanoparticles [11–16]. One of the methods to achieve a hydrophilic nanoparticle in polar solvent is transform the oil-soluble type into water-soluble type with post-treatment and functionalization of the surface. Some research groups have reported the surface modification techniques including surface exchange with cyclodextrin [11], copolypeptides [12], and interaction of surfactant [13]. Ligand exchange is a well-known method for tuning the surface properties of the nanoparticles. It involves adding an excess of ligand to the nanoparticle solution, which result in the displacement of the original ligand on the nanoparticle surface [14]. For example, Lattuada and Hatton [15] replaced the oleic groups coated on the iron oxide nanoparticle surfaces with various capping agents and produced reactive hydroxyl moieties through ligand-exchange reaction. This method was proposed a flexible methodology for the preparation of different kinds of monodisperse, hydrophilic magnetic nanoparticles. Generally speaking, a hydrophilic polymer or water-soluble ligand coating can reduce the aggregation and develop the colloidal stability of the magnetic nanoparticle in polar solvent. However, in some cases the polymer shell could significantly increase the overall size of the nanoparticles leading to a limited application [16].

To overcome this problem some research groups used one pot synthesis in polyol media without any surfactant [17,18]. Some other research groups used one pot synthesis for preparation of magnetic nanoparticle which is stable in polar solvent by using polymeric surfactant [19]. In this procedure they prepared magnetic nanoparticle using ethylene glycol as a solvent and poly

* Corresponding author.
E-mail address: moh_entezari@yahoo.com (M.H. Entezari).

0025-5408/$ – see front matter © 2013 Elsevier Ltd. All rights reserved.
http://dx.doi.org/10.1016/j.materresbull.2013.04.067

ethylene glycol as a surfactant. In some other cases, the additives like citrate group were used as hydrophilic ligand agent in the synthesis procedure [20,21].

In the synthesis approaches such as co-precipitation, water and hydroxyl ions have a strong affinity to ferric ions in the hydrolysis of ions under a proper molar ratio. So, the organic molecules have to compete with hydroxyl ions and water molecules and it is difficult to control the surface modification in aqueous solution. In the polyol media with no water involved in the reaction, the organic ligands can easily bind onto the particle surface via chemical bonds [22]. A combination of polyol media with an ultrasound can be a powerful method for the synthesis of hydrophilic magnetic nanoparticles. Sonochemistry is a novel and simple method for the synthesis of nanomaterial at the low temperature [23–29]. Ultrasound as an effective method is used for the synthesis of different compound under normal condition. The sonochemically synthesized materials are highly active in catalysis which is due to their particles size and high surface area [30]. The effects of ultrasound appear from acoustic cavitations, that is, the formation, growth and implosive collapse of bubbles in a liquid [31]. The implosive collapse of the bubbles generates a localized hot spot through adiabatic compression or shock wave formation within the gas phase of the collapsing bubble. The conditions formed in these hot spots have been experimentally determined, with transient temperatures of ~5000 K, pressure of 1800 atm and cooling rates in excess of 10^{10} K/s [31].

All of the mentioned research works have focused on the synthesis of nanoparticles dispersed in water and little works carried out on the stability of a magnetic alcosol (magnetic nanoparticle suspension in alcohol) [32]. Alcohol is a polar solvent which is commonly applied in material synthesis and biochemistry [33].

In this study, we report for the first time the combination of polyol media with ultrasonic irradiation to obtain magnetite nanoparticle which is stable in ethanol as a polar solvent. We used EG as polyol media without any surfactant. The EG act as hydrophilic solvent and hydrophilic assembler. The magnetite nanoparticles were obtained from aggregation of 2–3 nm primary nanoparticles as building blocks to produce secondary structure. Surface properties of primary nanoparticles are crucial for determination of final structure of secondary particles. It is suggested that organic ligands like EG with high binding affinities to primary nanoparticles can promote self-assembly. The growth of particles was attributed to the formation of magnetite nanoparticle nuclei and followed by the attachment and growth of primary building blocks and their Ostwald ripening process. Also, the effect of ultrasonic intensity was investigated to the synthesis of magnetite nanoparticles. It was found that the optimum intensity with high binding of EG on the surface of nanoparticles was 35 W/cm^2. The magnetite nanoparticles obtained under this condition have higher stability and dispersibility in ethanol as a polar solvent. The obtained magnetite nanoparticles were stable for more than12 months. This is attributed to the higher adsorbed EG and presence of OH groups on the surface of nanoparticle.

2. Experimental

2.1. Material

Iron (III) chloride·6H_2O, Iron (II) sulfate·7 H_2O, and Sodium hydroxide were purchased from Sigma–Aldrich. Absolute ethanol and Ethylene glycol anhydrous were purchased from Merck Company. Mili-Q water was used with a resistivity not less than 18.2 MΩ cm^{-1}.

Table 1
The preparation condition for magnetite nanoparticles.

No.	Intensity (W/cm^2)	Time (min)
1	51	30
2	44	30
3	35	30
4	24	30
5	35	60

2.2. Synthesis of magnetite nanoparticles

The synthesis of magnetite nanoparticle in EG as a polyol media was carried out as follows: 3.96 g of Iron (III) chloride.6H_2O and 2.04 g of Iron (II) sulfate.7 H_2O were dissolved in 50 mL of EG. The stock solution of 10 M NaOH/EG was prepared by dissolving NaOH in EG, the solution was heated for 1 h at 120 °C under ambient atmosphere. In a typical synthesis, a mixture of Fe(II) and Fe (III) in EG was poured in a completely washed and dried rosette cell as a reaction vessel. With start of sonication, 30 mL of NaOH/EG hot solution was added in the iron salts solution. The reaction turned black after addition of NaOH/EG. Then the solution was sonicated at 82 ± 2 °C for a proper time and intensity under air by using high-intensity ultrasonic horn (Ti-horn, 20 kHz). The temperature was held constant during the sonochemical process by a water jacket in a rosette cell. At the end of reaction, the final products were washed with mili-Q water and acetone several times to remove all basic impurities. Then, the obtained magnetic nanoparticles were dried at room temperature. The synthesis under different intensities was reported in Table 1. The intensity was obtained using calorimetry method.

2.3. Characterization and instrument

The size and morphology of the samples were characterized using TEM (CM30 philips, Netherlands, 150 kv). The sample was dispersed in ethanol and dropped on the copper grid before loading to the instrument. The X-Ray Diffractometer of product was recorded on Bruker, D8ADVANCE, Germany (X-Ray Tube Anode: Cu,Wavelength: 1.5406 Å (Cu Kα) Filter: Ni). The FTIR of the samples were recorded using Thermo Nicolet, Avatar 370 FTIR in the range of 400–4000 cm^{-1}. More detailed changes of the chemical structure were investigated using X-ray photoelectron spectroscopy (XPS) survey. XPS survey was carried out using a TWEEN ANODE XR3E2 X-ray photoelectron spectrophotometer with X-ray source. Thermogravimetric analysis was carried out for powder samples (30 mg) with a heating rate of 10 °C/min using a Mettler Toledo TGA thermogravimetric analyzer in N_2 atmosphere up to 700 °C. To determine the ξ potential, a proper amount of sample was dispersed in absolute ethanol by using high intensity ultrasonic irradiation (30%, 7 W/cm^2) for 30 min and then the dispersed solution was transferred to the cell of potential measurement. The ξ potential was determined with a Malven Zetasizer Nano ZS instrument. The colloidal stability of the magnetic suspension was studied by UV–visible spectrophotometer (Unico 2800) through monitoring the changes of the beam absorbance with time. The magnetic property of the nanoparticle was investigated using VSM (Vibrating sample magnetometer, Leckeshore model). The synthesis of nanomaterials and the dispersion of magnetite nanoparticles in ethanol were carried out with Sonics and Material, 750 W, 20 kHz.

2.4. Calorimetry

The real transducer's efficiency which is called acoustic power was determined by calorimetric method [28,29]. Since the

ultrasonic irradiation of a liquid produces heat, recording the temperatures as a function of time leads to the acoustic power estimation by the following equation:

$$P = mC_p\left(\frac{dT}{dt}\right) \quad (1)$$

where m is the mass of the sonicated liquid (g), C_p is the specific heat of medium (ethanol, 2.45 J (g K)$^{-1}$ and EG, 2.4 J (g K)$^{-1}$), and dT/dt is the temperature rise per second. Based on acoustic power (W), the ultrasonic intensity can be expressed in watt per unit area of the emitting surface (W/cm^2).

3. Results and discussion

The sono-synthesis of magnetite nanoparticles which are stable in ethanol as polar solvent is discussed in detail. In this work, EG was used as a polyol medium and hydrophilic organic assembler. The magnetic alcosol was stable for more than 12 months. The stability of alcosol, the analysis, and the characterization of magnetic nanoparticles describe as follows:

3.1. Stability of suspension

To determine the colloidal stability of magnetite nanoparticle in ethanol, a proper amount of magnetite nanoparticles (2 mg) was dispersed in 50 mL of absolute ethanol. The suspension was irradiated by ultrasound at 30% (7 W/cm^2) in 30 min of aging time.

The colloidal stability of magnetic suspension was measured by monitoring the changes of the absorbance by passing the beam through the cell. The measurement was carried out at the wavelength of 250 nm. The changes of the effective beam absorbance were monitored for more than 12 months. In the first month, the stability of suspension was controlled in short times. The evolution of normalized beam absorbance with time is shown in Fig. 1 where the absorbance A was normalized by dividing to the initial absorbance A_0. A significant decrease in the absorbance was observed for some samples during the first stage. It is suggested that this observation is due to the precipitate of unmodified magnetite nanoparticles in ethanol. When two unmodified nanoparticles collide with each other during Brownian motion, the van der Waals force between nanoparticles can cause to aggregation and precipitation. The same behavior was observed by another research group [32]. The intensity of ultrasound and the time of sonication applied for the preparation of the suspension were very important. According to the Fig. 1, the sample No. 3 showed a highest stability than the others. This confirms that the sample No. 3 was irradiated under optimum conditions in point of intensity and the time of sonication for the adsorption of EG molecules on the surface of nanoparticles. It is proposed that the interaction between EG and nanoparticle could not be very high. Because, at higher intensity and longer aging times (sample No. 5) the colloidal system was not stable. It seems that under this condition, the absorbed EG molecules on the nanoparticles were desorbed. There are two crucial parameters about the EG coating on the surface of nanoparticles. Increase of mass transfer due to action of shock waves and microjets and corrosion of surface due to collapse of bubble near the surface. Therefore, predominant factor determine the amount of EG coating on the surface. In the higher intensity and longer times the corrosion of surface can desorbed the EG molecules from the surface. Furthermore, the lower intensity (40%) cannot provide stable coating on the surface of the nanoparticles.

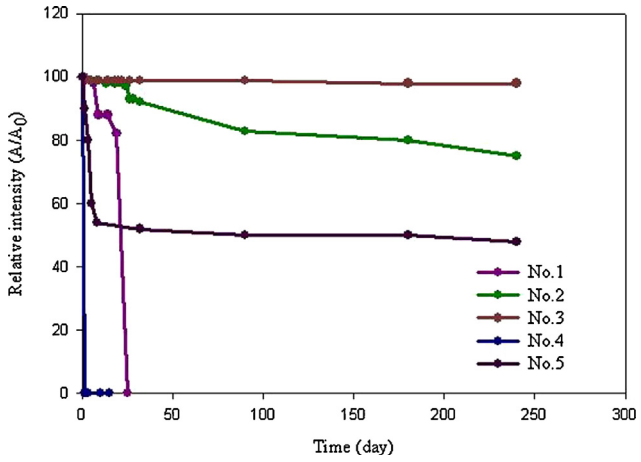

Fig. 1. The colloidal stability of the magnetic suspension in ethanol at different condition.

A snapshot of the magnetic suspensions was shown in Fig. 2a. This image was recorded one month after preparation for the samples No. 1 and 3. As it is shown, the nanomagnetic particles were precipitated in sample No. 1and in case of sample No. 3, the suspension was stable. A suspension with a yellow color represents the stabilization of the nanomagnet in the medium. In Fig. 2b, a proposed surface modification of the nanoparticle by EG is shown.

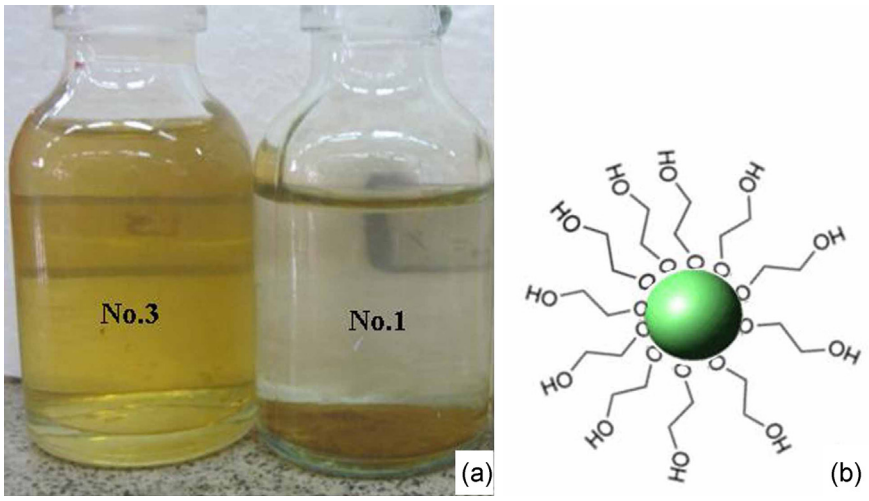

Fig. 2. (a) Snapshot of the sample No. 1 and No. 3 after 1 month and (b) the proposed surface modified of magnetite nanoparticles with EG molecules.

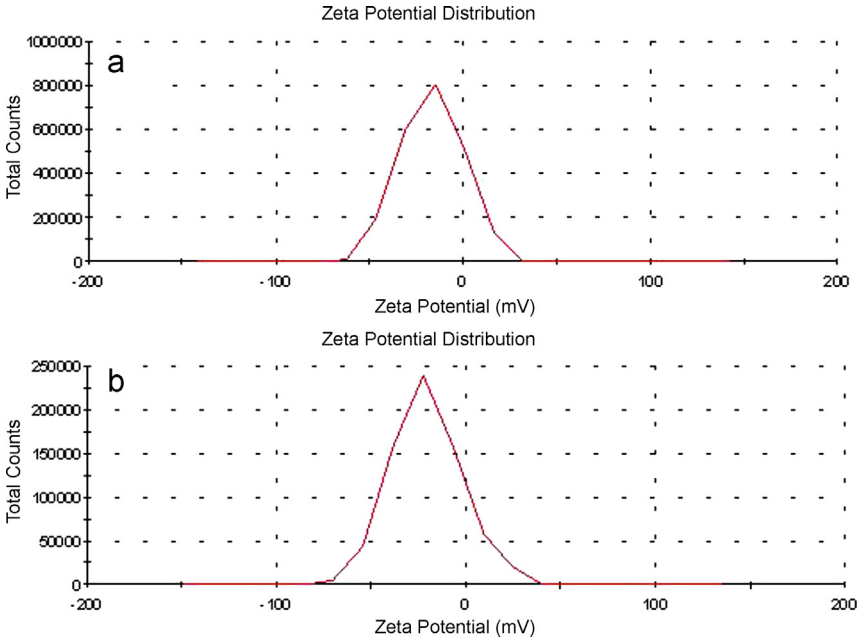

Fig. 3. The ξ potential amount of magnetite nanoparticle in ethanol which obtained with sample No. 3 (a) immediately after dispersion and (b) after 2 months.

Due to a higher stability of sample No. 3 than other samples, the experiments and analyses were focused on this sample.

The ξ potential measurement is important for understanding the dispersion behavior of the nanoparticles in a liquid medium. The greater the ξ potential, the more stable suspension [33]. Fig. 3 shows the change of ξ potential for the suspension of magnetite nanoparticle in ethanol obtained immediately and after 2 months of preparation with sample No. 3. The average ξ potential of suspensions were −17 mV and −21 mV, respectively. Based on these results, the surface of nanoparticles is negatively charged. It is assumed that the negatively charge can be due to partial ionization of adsorbed EG on the surface of nanoparticles. The electrostatic repulsion forces between particles lead to more free particles and decrease the particle coagulation. But, it seems that the ξ potential is not sufficiently high to warrant colloidal stability and the surface properties of nanoparticles should be involved to such a high stability.

3.2. Crystallite structure, particle size, and magnetic properties

The crystallite structure for sample No. 3 was carried out by powder X-ray diffraction (XRD). As showing in Fig. 4, it reveals that the XRD peaks of the original phase in the pattern can be indexed to the (2 2 0), (3 1 1), (4 0 0), (5 1 1), and (4 4 0) for the face centered cubic magnetite structure in accordance with JCPDS card of Fe_3O_4 (JCPDS-19-0629).

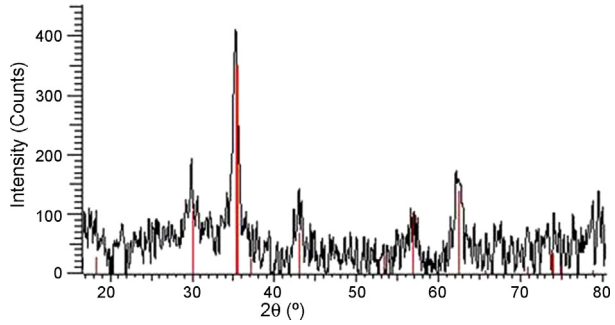

Fig. 4. The XRD diffraction pattern of magnetite nanoparticles (sample No. 3).

The size, size distribution and SAED pattern of magnetite nanoparticles in sample 3 is shown in Fig. 5. According to this image, the average size is 24 nm and the nanoparticles contain primary nanoparticles with average size of 2–3 nm. The TEM confirms that the secondary structures are composed of smaller building blocks. It is suggested that the EG acts as an organic binder to assemble primary nanoparticles. The bridging between building blocks occurs via EG adsorbed on the surface of the nanoparticles. Such structure and morphology was reported in the literature [34]. The selected area electron diffraction pattern (SAED) of the nanoparticles is shown in Fig. 5d. The SAED exhibits polycrystalline pattern. In addition, the size distribution of secondary nanoparticles is presented in Fig. 5e.

The magnetic properties of the sample No. 3 were investigated by vibrating sample magnetometer (VSM). Fig. 6 shows the room temperature magnetization versus applied field. The curve obtained at 300 K was between −7 and 7 kOe. The saturation magnetization at this temperature was 56 emu/g and no coercivity was observed which confirms the superparamagnetic behavior and single domain of the sample.

3.3. Surface study

The FTIR analysis further identified the organic coating on the surface of the magnetite nanoparticles. Fig. 7 and Table 2 show the spectra and infrared transmission frequencies of EG molecule and final products. As shown in Table 2 and Fig. 7, the peaks around 550–620 cm^{-1} in all samples are due to M–O vibration band. The characteristic peak of EG at 1459 cm^{-1} (CH_2 bending) and two peaks at 1043 cm^{-1} and 1087 cm^{-1} (C–O symmetric stretching) appear in the spectrum of the products except for the samples No. 4 and No. 5. This indicates that EG can be presented on the surface of magnetite nanocrystal (samples No 1–3). The peak at 1043 cm^{-1} for the pure EG showed a red shift (increased wavelength) in the product which confirms the interaction between EG and surface of magnetite nanoparticle via C–O group. In the case of No. 4 and No. 5, no peaks related to the EG molecules are observed which confirms the less adsorbed EG molecules on the surface of nanoparticles. This observation indicates that the intensity of ultrasonic irradiation is a crucial parameter for the adsorption

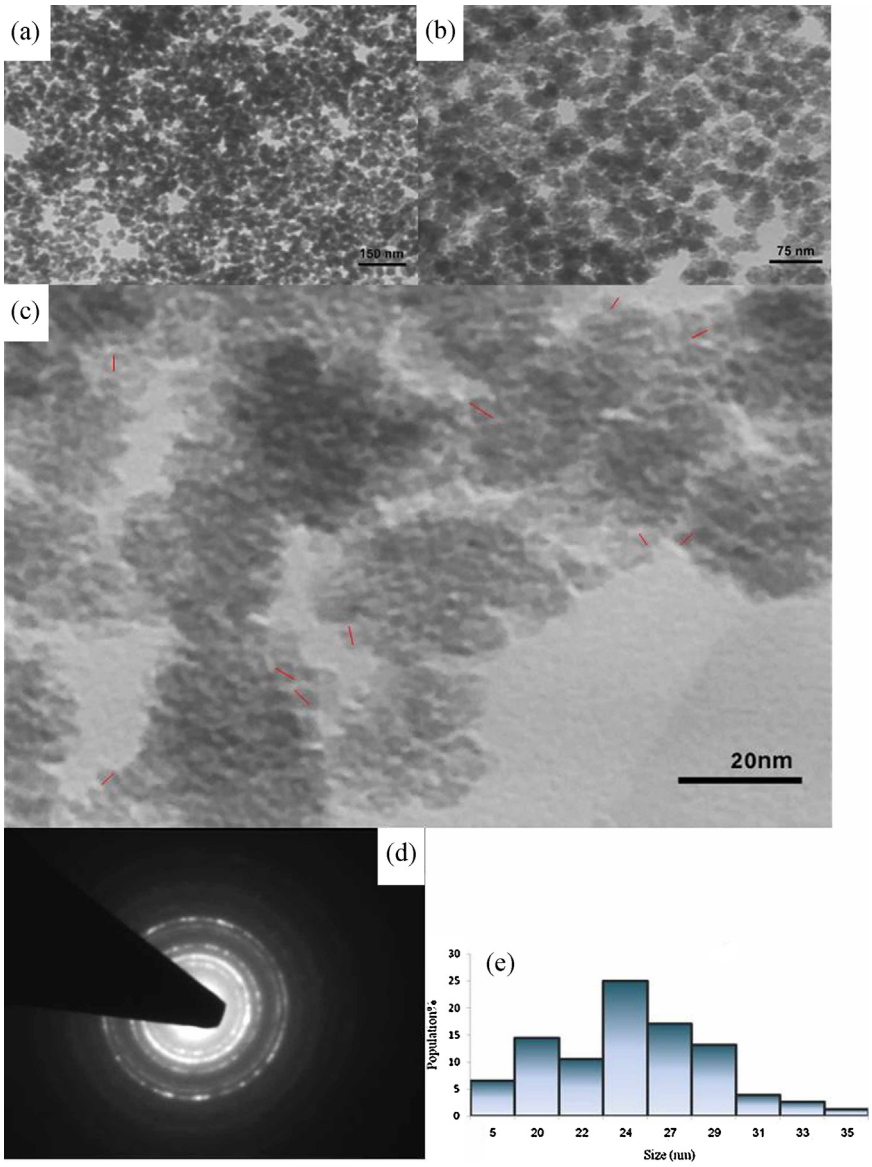

Fig. 5. (a–c) TEM images of magnetite nanoparticles, (d) SAED pattern, and (e) histogram showing the particle size distribution measured from Fig. 5a,b (sample No. 3).

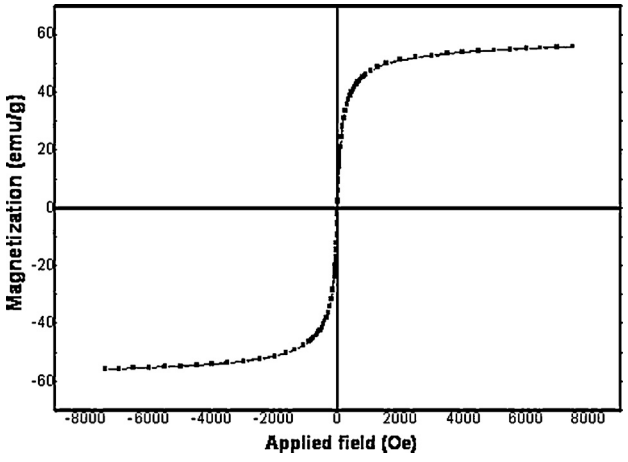

Fig. 6. Hysteresis cycle of the magnetization of the sample No. 3.

of EG on the surface of nanoparticles. A higher amount of adsorbed EG on the surface of magnetite nanoparticles led to more stable of nanoparticles in the ethanol (No. 3).

Fig. 8 and Table 3 show the most important IR vibrations before and after dispersion of nanomagnetic particles in ethanol for the sample No. 3 in comparison with ethanol and EG. The peaks related to OH bands for the sample No. 3 before dispersion, EG, ethanol and the sample No. 3 after dispersion in ethanol are observed at 3396 cm^{-1}, 3426 cm^{-1}, 3347 cm^{-1}, and 3353 cm^{-1}, respectively. It is assumed that the hydrogen bonding between OH groups in ethanol and adsorbed EG molecules on the surface of magnetite nanoparticles is responsible for the observed shift. In addition of ξ potential, the enhanced stability of dispersion could be attributed to the solvation of adsorbed EG molecules on the surface of magnetite nanoparticles.

The XPS (X-ray photoelectron spectroscopy) for the sample No. 3 is presented in Fig. 9. The peak indicating at ~710 eV was assigned to the Fe–O band and the observed position is consistent with the literature [35–37]. The carbon spectrum of the coated magnetite nanoparticles is presented as two peaks at 284 eV (C–C

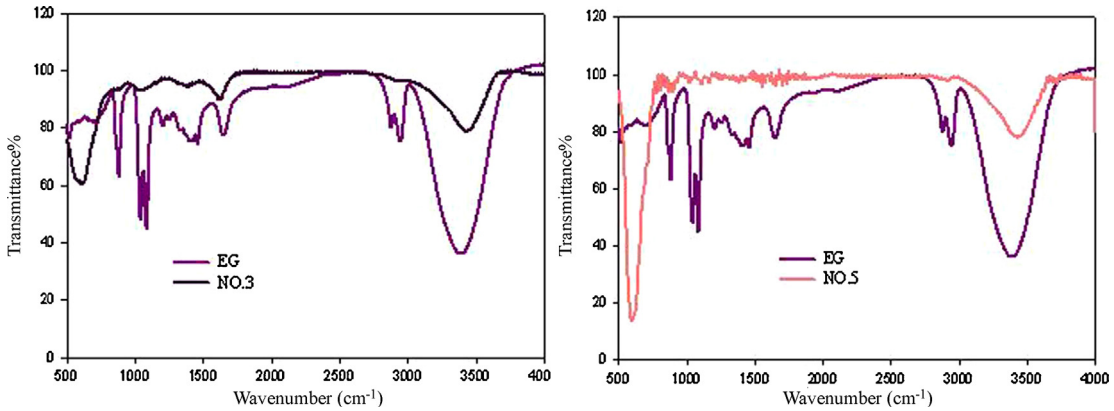

Fig. 7. FTIR spectra of pure EG and coated magnetite nanoparticles.

Table 2
Infrared transmission frequencies of pure EG and final products.

Observed bands (cm^{-1})						
EG	No. 1	No. 2	No. 3	No. 4	No. 5	Band assignment
3396	3420	3360	3426	3370	3380	ν O–H and adsorbed water
2881, 2946	2870, 2930	2810	2931	–	–	(ν_S, ν_{as}) CH_2
1646	1640	1600	1617	1590	–	δ H_2O
1459	1400	1350	1413	–	–	CH_2 bending
1043–1087	1030	1010	1033	–	–	ν C–O
–	620	550	620	560	590	ν M–O

Table 3
Infrared transmission frequencies of sample No. 3 before and after dispersion in ethanol in compare with ethanol and EG.

Observed bands (cm^{-1})				
EG	No. 3	No. 3 dispersed in ethanol	Ethanol	Band assignment
3396	3426	3353	3347	ν O–H and adsorbed water
2881, 2946	2931	2900–2973	2927–2975	(ν_S, ν_{as}) CH_2
1646	1617	1654	1658	δ H_2O
1459	1413	1380	1380	CH_2 bending
1043–1087	1033	1051–1089	1057–1087	ν C–O
–	620	620	–	ν M–O

band) and at 287 eV (C–O band). It is suggested that the C–C and C–O peaks originated from the EG molecules which coated on the surface of magnetite nanoparticles. The peak located at 530 eV can be assigned to Fe–O band.

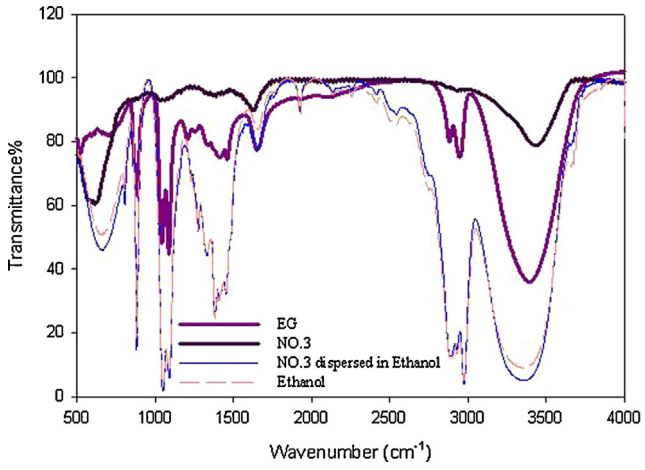

Fig. 8. FTIR spectra of sample No. 3 before and after dispersion in ethanol in compare with pure EG and ethanol.

The presence of polyol ligands on the surface of the magnetite nanoparticles is supported by TGA analysis. Fig. 10 shows the TGA analysis curves of the samples No. 3 and No. 4. In the case of No. 3, there are three weight losses from room temperature to 700 °C. The initial weight loss from room temperature to 230 °C was attributed to the loss of surface adsorbed water and residual free EG. The second and third weight losses are in the ranges of 230–380 °C and 410–700 °C. Most probably, these losses are due to the desorption of EG attached to the surface of magnetite nanoparticles. The total weight loss in this case was 14%. Some researchers explained that the TGA behaviors are based on the bi-layer adsorbed models on the particle surface [38,39], while others claimed that the double-stepped TGA curve is due to two different kinds of binding sites [40,41]. Based on TGA results, it seems that the TGA curves for sample No. 3 is in agreement with the two different binding sites on the surface of the nanoparticles. The second weight loss is much higher than the third one. This means that the concentration of adsorbing species with strong interaction is much lower than the concentration with lower interaction. In the case of sample No. 4, two weight losses are observed. The first weight loss occurred from room temperature to 83 °C which is due to the adsorbed water and the second weight loss occurred in the range of 83–570 °C which is originated from the adsorbed EG molecules on the surface of nanoparticles. The amount of total weight loss was about 10% and the third weight loss mostly

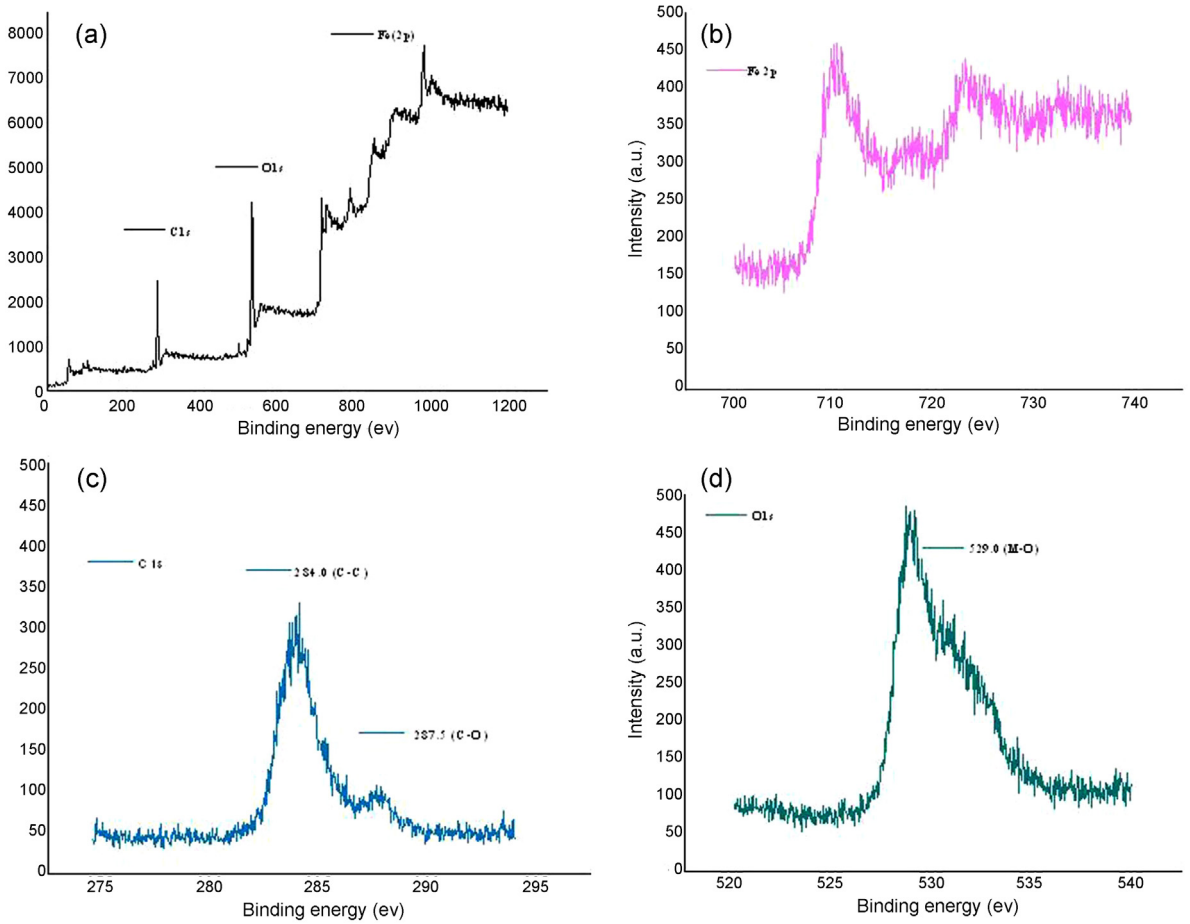

Fig. 9. XPS spectrums that corresponds to (a) whole spectrum, (b) Fe2p, (c) C1s, and (d) O1s.

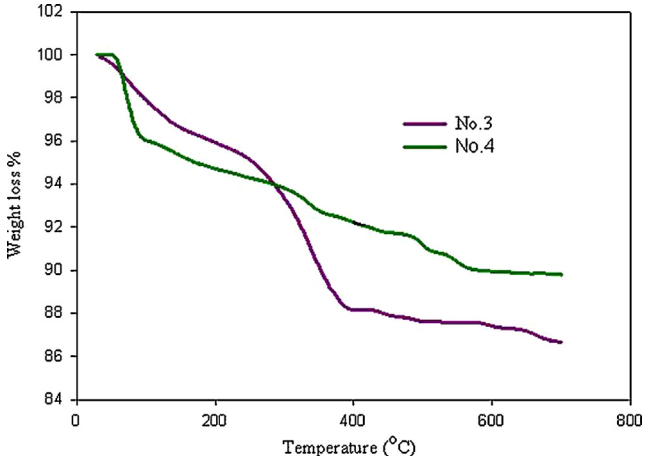

Fig. 10. TGA curve of magnetite nanoparticles for sample No. 3 and No. 4.

disappeared. This observation confirms that the ultrasonic intensity is a crucial parameter for the adsorbed organic species on the surface of nanoparticles. It is obvious that the maximum stability is due to the maximum adsorbed EG molecules on the surface of the magnetic nanoparticles.

4. Conclusion

In summary, we have developed a facile approach to prepare hydrophilic magnetite nanocrystal in polyol liquid via ultrasonic irradiation at relatively low temperature. The stability of magnetite nanoparticles in ethanol as polar solvent was investigated. This approach has several advantageous. (1) No surfactant was used in this process, (2) the in situ preparation of magnetite nanoparticles with hydrophilic surface, (3) the reaction was run at low temperature compared to the other polyol process, (4) the hydrophilic magnetite nanoparticles easily dispersed in water and the other polar solvent, and (5) the obtained magnetite nanoparticles were stable in ethanol even after 12 months.

Based on the experimental results, the magnetite nanoparticles with average size of 24 nm were composed of small building blocks with average size of 2 nm and exhibited a spherical structure. The EG as polyol solvent with high binding affinity to primary building blocks promotes the self-assembly by adsorption on the surface of magnetite nanoparticles. Also, the results showed that the ultrasonic intensity was a crucial parameter to obtain hydrophilic nanoparticles. Therefore, this method offers an effective and facile route to replace the traditional co-precipitation method for the preparation of superparamagnetic and hydrophilic magnetic nanoparticle.

References

[1] J.Y. Park, P. Daksha, G.H. Lee, S. Woo, Y. Chang, Nanotechnology 19 (2008) 1–7.
[2] M.H. Sousa, J.C. Rubim, P.G. Sobrinho, F.A. Tourinho, J. Magn. Magn. Mater. 225 (2001) 67–72.
[3] R. Ganguly, A.P. Gaind, S. Sen, I.K. Puri, J. Magn. Magn. Mater. 289 (2005) 331–334.
[4] F. Hu, L. Wei, Z. Zhou, Y. Ran, Z. Li, M. Gao, Adv. Mater. 18 (2006) 2553–2556.
[5] T. Black, K. Raj, S. Tsuda, J. Magn. Magn. Mater. 252 (2002) 39–42.
[6] Z.J. Zhang, Z.L. Wang, B.C. Chakoumakos, J.S. Yin, J. Am. Chem. Soc. 120 (1998) 1800–1804.
[7] S. Si, C. Li, X. Wang, D. Yu, Q. Peng, Y. Li, Cryst. Growth Des. 5 (2005) 391–393.

[8] T. Hyoen, Chem. Commun. 8 (2003) 927–934.
[9] Q. Song, Z.J. Zhang, J. Am. Chem. Soc. 126 (2004) 6164–6168.
[10] S. Sun, H. Zeng, D.B. Robinson, S. Raoux, P.M. Rice, S.X. Wang, G. Li, J. Am. Chem. Soc. 126 (2004) 273–279.
[11] Y. Wang, J.F. Wong, X. Teng, X.Z. Lin, H. Yang, Nano Lett. 3 (2003) 1555–1559.
[12] L.E. Euliss, S.G. Grancharov, S. O'Brien, T.J. Deming, G.D. Stucky, C.B. Murray, G.A. Held, Nano Lett. 3 (2003) 1489–1493.
[13] T. Pellegrino, L. Manna, S. Kudera, T. Liedl, D. Koktysh, A.L. Rogach, S. Keller, J. Rädler, G. Natile, W.J. Parak, Nano Lett. 4 (2004) 703–707.
[14] W. Wu, Q. He, C. Jiang, Nanoscale Res. Lett. 3 (2008) 397–415.
[15] M. Lattuada, T.A. Hatton, Langmuir 23 (2007) 2158–2168.
[16] F.-Y. Cheng, C.-H. Su, Y.-S. Yang, C.-S. Yeh, C.-Y. Tsai, C.-L. Wu, M.-T. Wu, D.-B. Shieh, Biomaterials 26 (2005) 729–738.
[17] W. Cai, J. Wan, J. Colloid Interface Sci. 305 (2007) 366–370.
[18] H. Yang, C. Zhang, X. Shi, H. Hua, X. Du, Y. Fang, Y. Mad, H. Wu, S. Yang, Biomaterials 31 (2010) 3667–3673.
[19] H. Deng, X. Li, Q. Peng, X. Wang, J. Chen, Y. Li, Angew. Chem. Int. Ed. 44 (2005) 2782–2785.
[20] J. Ge, Y. Hu, M. Biasini, W.P. Beyermann, Y. Yin, Angew. Chem. Int. Ed. 46 (2007) 4342–4345.
[21] J. Liu, Z. Sun, Y. Deng, Y. Zou, C. Li, X. Guo, L. Xiong, Y. Gao, F. Li, D. Zhao, Angew. Chem. Int. Ed. 48 (2009) 5875–5879.
[22] X. Lu, M. Niu, R. Qiao, M. Gao, J. Phys. Chem. B 112 (2008) 14390–14394.
[23] M. Sivakumar, A. Towata, K. Yasui, T. Tuziuti, Y. Iida, Curr. Appl. Phys. 6 (2006) 591–593.
[24] W.H. Suh, K.S. Suslick, J. Am. Chem. Soc. 127 (2005) 12007–12010.
[25] R.A. Caruso, M. Ashokkumar, F. Grieser, Colloids Surf. A 169 (2000) 219–225.
[26] A. Pradhan, R.C. Jones, D. Caruntu, C.J. O'Connor, M.A. Tarr, Ultrason. Sonochem. 15 (2008) 891–897.
[27] T. Rohani Bastami, M.H. Entezari, Chem. Eng. J. 164 (2010) 261–266.
[28] T. Rohani Bastami, M.H. Entezari, Ultrason. Sonochem. 19 (2012) 560–569.
[29] T. Rohani Bastami, M.H. Entezari, Ultrason. Sonochem. 19 (2012) 830–840.
[30] V. Kesavan, P.S. Sivanand, S. Chandrasekaran, Y. Koltypin, A. Gedanken, Angew. Chem. Int. Ed. 38 (1999) 3521–3523.
[31] J.H. Bang, K.S. Suslick, Adv. Mater. 22 (2010) 1039–1059.
[32] S.-Y. Lee, M.T. Harris, J. Colloid Interface Sci. 293 (2006) 401–408.
[33] X.-J. Wang, X. Li, S. Yang, Energy Fuels 23 (2009) 2684–2689.
[34] T. Rohani Bastami, M.H. Entezari, Q.H. Hua, S. Budi Hartono, S.Z. Qiao, Chem. Eng. J. 210 (2012) 157–165.
[35] R. Abu Mukh-Qasem, A. Gedanken, J. Colloid Interface Sci. 284 (2005) 489–494.
[36] U. Schwertmann, R.M. Cornell, Iron Oxides in the Laboratory: Preparation and Characterization, second ed., VCH, Weinheim, New York, 2000.
[37] C.W. Jung, Magn. Reson. Imaging 13 (1995) 675–691.
[38] A. Swami, A. Kumar, M. Sastry, Langmuir 19 (2003) 1168–1172.
[39] Y. Sahoo, H. Pizem, T. Fried, D. Golodnitsky, L. Burstein, C.N. Sukenik, G. Markovich, Langmuir 17 (2001) 7907–7911.
[40] C. Yee, G. Kataby, A. Ulman, T. Prozorov, H. White, A. King, M. Rafailovich, J. Sokolov, A. Gedanken, Langmuir 15 (1999) 7111–7115.
[41] L. Zhang, R. He, H.-C. Gu, Appl. Surf. Sci. 253 (2006) 2611–2617.